Electronic Supplementary Information to

Silica@zirconia@poly(malic acid) nanoparticle: a promising nanocarrier for theranostic applications

in Journal of Materials Chemistry B

Lívia Naszályi Nagy[1,*](✉), Andras Polyak[2,3], Judith Mihály[1], Ágnes Szécsényi[1,†], Imola Cs. Szigyártó[1], Zsuzsanna Czégény[1], Emma Jakab[1], Péter Németh[1], Balázs Magda[4], Pál Szabó[4], Zsuzsanna Veres[4], Katalin Jemnitz[4], Imre Bertóti[1], Róbert Péter Jóba[5], György Trencsényi[6], Lajos Balogh[2], Attila Bóta[1]

[1] Institute of Materials and Environmental Chemistry, Research Centre for Natural Sciences, Hungarian Academy of Sciences (IMEC RCNS HAS), Budapest H-1117, Hungary, nagy.naszalyi.livia@ttk.mta.hu

[2] Department of Radiobiology, National Research Institute for Radiobiology and Radiohygiene (NRIRR), Budapest H-1221, Hungary

[3] Department of Nuclear Medicine, Hannover Medical School, Hannover, Carl-Neuberg-Str 1, D-30625, Germany

[4] Institute of Organic Chemistry, Research Centre for Natural Sciences, Hungarian Academy of Sciences (IOC RCNS HAS), Budapest H-1117, Hungary

[5] Department of Nuclear Medicine, Semmelweis University, Budapest H-1082, Hungary

[6] Department of Nuclear Medicine, University of Debrecen, Debrecen H-4032, Hungary

Characterization

Dynamic light scattering measurements

Table S-1 Na_2HPO_4 buffer concentrations after addition of NaCl electrolyte.

NaCl (mM)	Na_2HPO_4 concentration (mM)					
0	0	10	30	50	70	90
19.3	0	8	24	40	56	72
38.5	0	6.7	20	33.3	46.7	60
57.8	0	5.7	17.1	28.6	40	51.4
77	0	5	15	25	35	45

X-ray photoelectron spectroscopy measurements

The pressure of the analysis chamber was lower than 1×10^{-7} Pa. Wide scan spectra were recorded for all samples in the 100-1300 eV kinetic energy range using 80 eV pass-energy, with 0.5 eV steps and 0.5 s dwell time. High-resolution spectra of photoelectron lines of the main constituent elements, and the C1s region for the carbon-containing layers and contaminations, were recorded at 40 eV pass-energy by 0.1 eV steps and min. 1 s dwell time.

Chemical shifts, representing different bonding states of the O1s, C1s Zr3d and Si2p spectra, were evaluated by applying peak decomposition procedure, by fitting the measured peak envelope with Gauss-Lorentz (70:30) type components (of 1.7-2 eV half-widths), using the Kratos Vision 2 software.

Quantitative analysis, based on peak area intensities (after removal of the Shirley- or linear-type

* Present address: MTA-SE Molecular Biophysics Research Group, Budapest, Tűzoltó Str 37-47, H-1094, Hungary. E-mail: lnaszalyi@gmail.com

† Present address: Department of Chemical Engineering, Delft University of Technology, Delft 2600 AA, The Netherlands

background), was performed by the Vision 2000 program using experimentally determined photo-ionisation cross-section data and provided by the manufacturer of the spectrometer.

Mass spectrometry

Calibrating solutions of malic acid were prepared in MQ water (1.3×10^{-3} – 1.3×10^{-6} M).
Chromatography was performed using a Perkin Elmer Series 200 micro LC system with Series 200 Autosampler. Chromatographic separation was achieved using a Purospher Star RP-18 endcapped (Merck, Germany) column (55×2 mm, 3 μm) with a C18 4×2 mm Security Guard Cartridge (Phenomenex, USA). Mobile phase A was water with 0.1% formic acid and mobile phase B was acetonitrile with 0.1% formic acid. For the MS/MS analysis, a QTrap 3200 system with a TurboIon-Spray source (AB Sciex, USA) was used. Flow rate was set to 0.4 ml/min and gradient elution was programmed as follows: 5% eluent B from 0 to 1.5 min; from 1.5 to 3 min linear increase to 95% eluent B; from 3 to 6 min 95% eluent B is retained; from 6 to 6.5 min back to initial conditions with 5% eluent B. The injected volume was 10 μl. Multiple Reaction Monitoring (MRM) analysis was done using the electrospray source in negative ion mode. The specific precursor-to-ion transitions monitored were m/z 133 → 115. The collision energy was -14 eV.

Cell viability experiments

The MTT assay was used to establish the cytotoxicity of CN nanoparticles. At 24 h after seeding, hepatocytes were treated with various concentrations (10-500 μg/ml) of CN or the vehicle (0.1% DMSO) as control for 24 h. Then the cells were washed and assayed or incubated for 24 h longer without CN, respectively. Next, MTT (1 mg/ml) was added to each well and incubated at 37 °C for 2 h. The supernatant was discarded and the formazan precipitates were dissolved in DMSO. After dissolution, absorbance was measured at 540 nm on a microplate reader (Molecular Devices LLC). Background absorbance of the medium without cells was subtracted from all experimental samples. Viability data are expressed as Mean ± SD percentage of the vehicle treated wells. All experiments were carried out using 4 wells/treatment groups.

Labelling efficiency and stability

Radiochemical purity of the ^{99m}Tc-labelled nanocarrier was examined by means of thin-layer chromatography (TLC) using silica gel as the coating substance on glass-fibre sheets (ITLC-SG). Plates were developed in methyl ethyl ketone. Free, unbound ^{99m}Tc-pertechnetate migrated with the solvent to the front line (R_f=1), while the labelled compound was located at the origin (R_f=0). A Raytest MiniGita instrument (Mini Gamma Isotope Thin Layer Scanner) was applied to determine the distribution of radioactivity in the developed ITLC-SG plates. Labelling efficiency was examined 1 h, 4 h and 20 h after labelling. To preclude the presence of colloid sized precipitate or other post-labelling contaminants, the labelled nanocarrier was also examined with a Malvern Zetasizer Nano ZS instrument (Malvern, Worcs, UK).

***In vivo* tumor model**

In vivo experiments were carried out 12±1 days after subcutaneous injection of tumour cells. Tumor growth was assessed by caliper measurements.
Laboratory animals were kept and treated in compliance with all applicable sections of the Hungarian Laws No. XXVIII/1998 and LXVII/2002 on the protection and welfare of animals and animal welfare directions and regulations of the European Union. The Governmental Ethical Committee approved the study (permission No. 22.1/609/001/2010). The experimental protocol was approved by the Laboratory Animal Care and Use Committee of the University of Debrecen.

Results

TEM pictures of the inorganic core

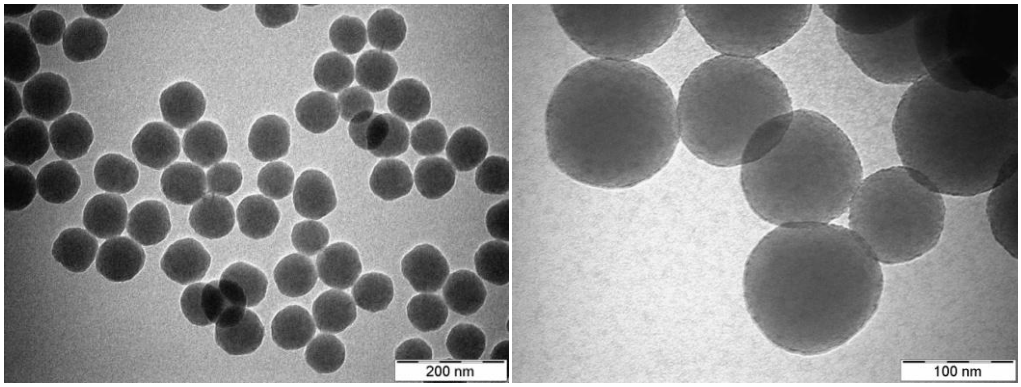

Fig.S-1 TEM images of SiO_2 (left) and SiO_2@ZrO_2 (right) inorganic core. The surface of the latter is rough showing the deposition of small ZrO_2 crystallites.

Structure and colloid stability of complex nanocarriers

Intensity-weighted Z-average diameters are 121 nm (SiO_2 sol, PdI: 0.122), 146 nm (SiO_2@ZrO_2 sol, PdI: 0.088) and 266 nm (CN suspension, PdI: 0.263).

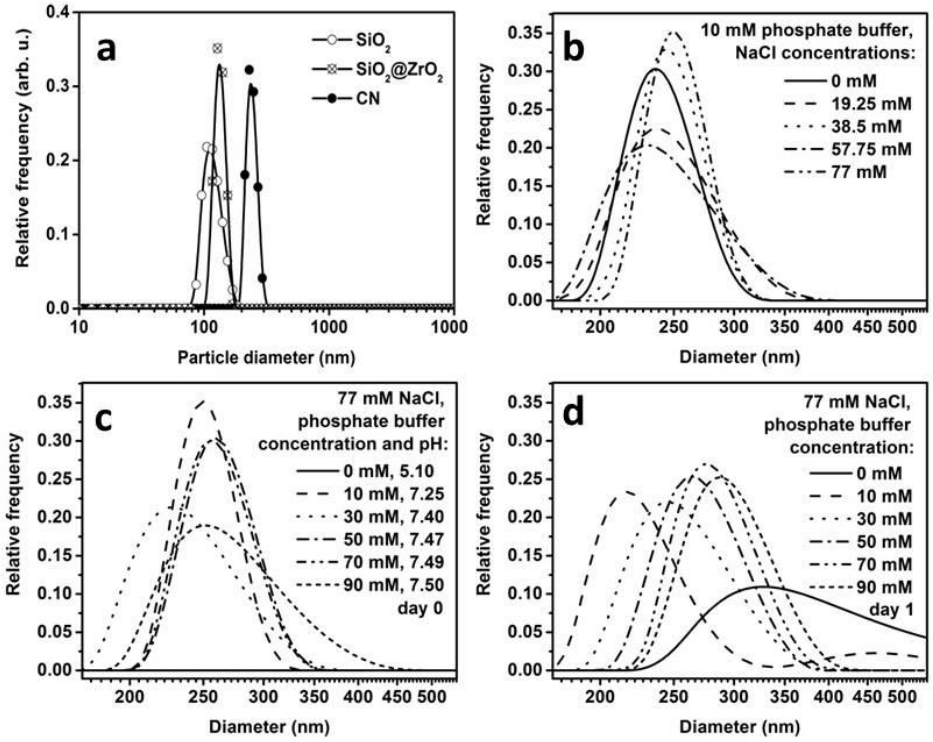

Fig.S-2 Size distribution functions of a) the SiO_2 sol and the core@shell SiO_2@ZrO_2 sol in ethanol and the complex nanocarriers (CN) in 10 mM phosphate buffer and b-c-d) 0.5 mg/ml CN suspensions of various phosphate buffer and saline content. Destabilization can mainly be observed after one day at higher buffer content or without any buffer (acidic pH).

Characterization of the polymeric shell

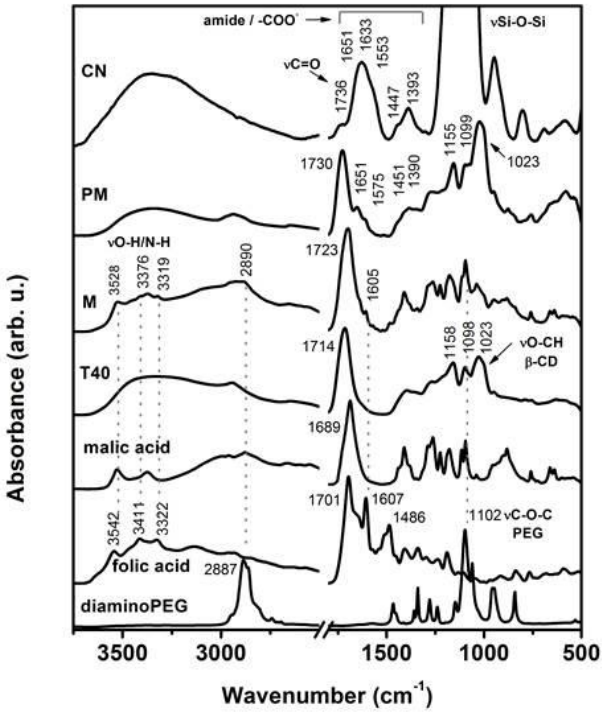

Fig.S-3 FTIR analysis of polymeric shell components, their physical mixture (M), their bulk polymerization product (PM) and CN particles.

According to the differential thermal curve (Fig.S-3), small-scale dehydration takes place below 120°C. Above 130°C begins the degradation of polymeric shell components of the physical mixture (M) with peaks at 210°C, 270°C (main peak) and 400°C. After polymerization of the mixture (PM), a main peak appears at 350°C and the original peaks are present with a lowered intensity and shifted to higher temperatures (240°C, 275°C).

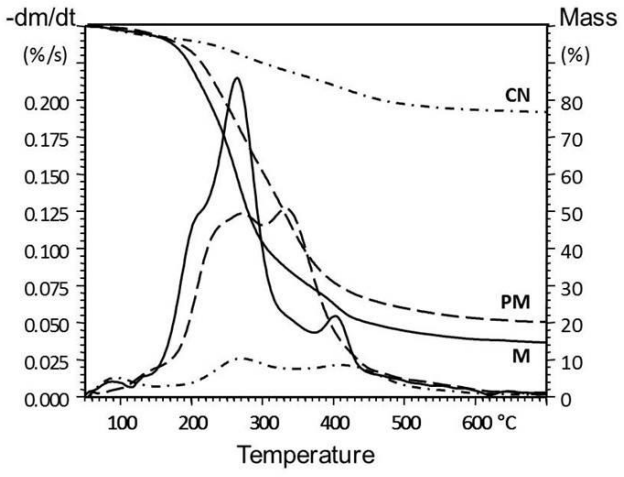

Fig.S-4 TG and DTG curves of the physical mixture of polymer components (solid line), the bulk polymerization product of polymer components (dashed line) and CN (dashed-dotted line). The weight loss of samples at 700°C is: 23 m/m% for CN, 79% for M and 85% for PM.

The peak at 400°C disappears from the DTG curve of the polymerized mixture showing the participation of highly stable component in the network. The DTG curve of CN particles shows a different polymeric composition than PM, since we observe two main peaks at 270°C and at 410°C.).

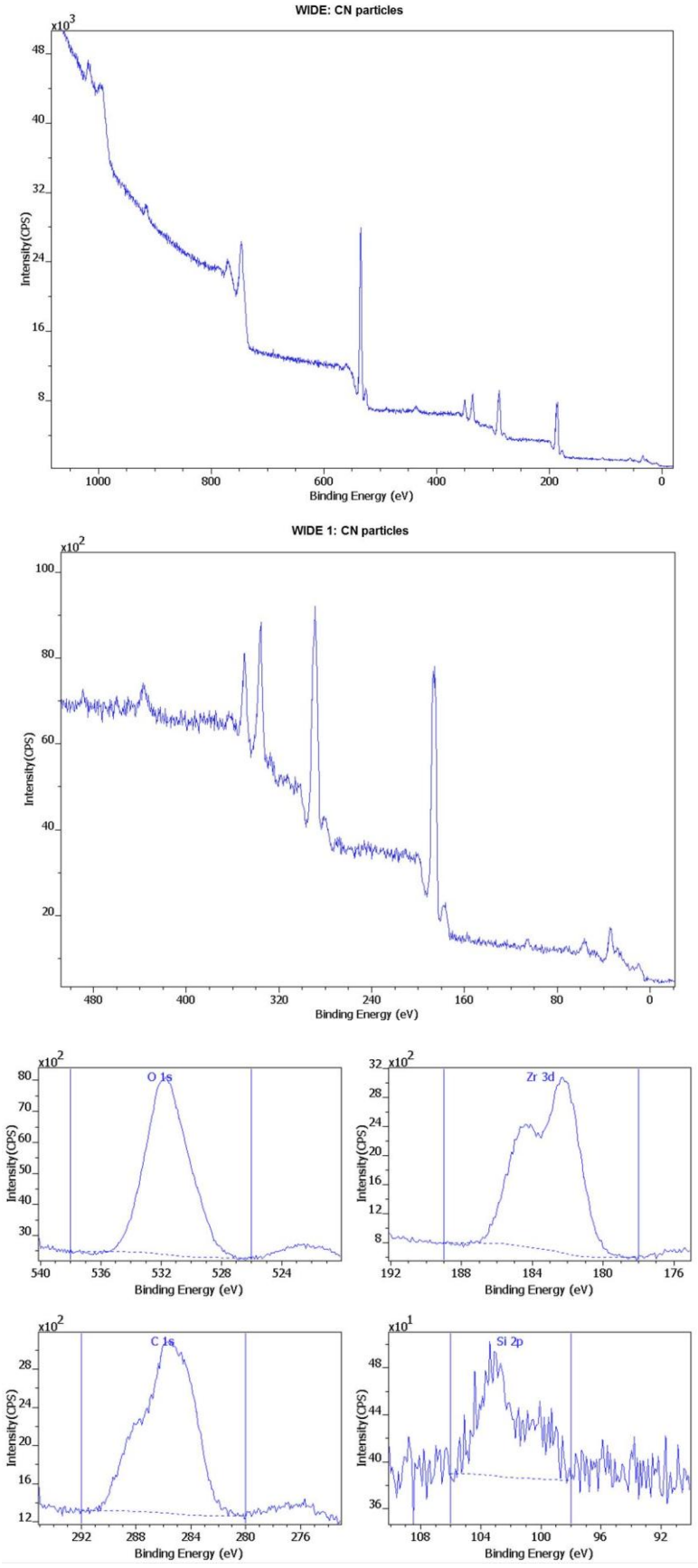

Fig.S-5 Raw XPS curves of CN nanoparticles.

Table S-2 Experimental (from XPS) and theorethical composition of the polymeric shell and single components (in atomic ratio)

	C (at. %)	O (at. %)	N (at. %)
experimental	65.6	34.4	-
theorethical	53.2	45.4	1.4
without folic acid (FA)	52.8	47.1	0.1
without FA and PEG	51.9	48.1	0.0
T40 polymer	52.5	47.5	0.0
malic acid	44.4	55.6	0.0
folic acid	59.4	18.7	21.9
diaminoPEG	66.7	31.9	1.4
beta-CD	54.6	45.4	0.0

Degradation of the polymeric shell

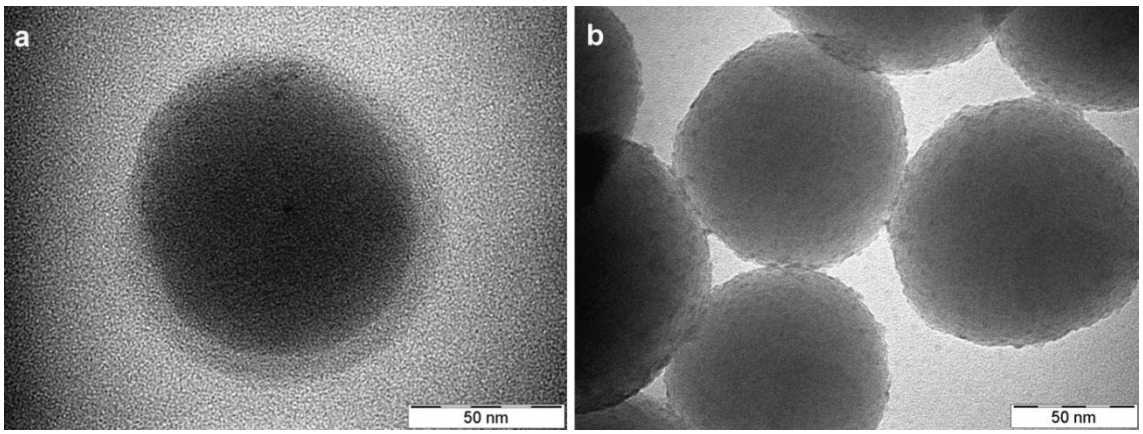

Fig.S-6 TEM pictures of nanoparticles with copolymer shell built up from L-(-)-malic acid and β-cyclodextrin monomers with the addition of diamino-PEG and folic acid for the last 10 min. of the polymerization reaction a) before and b) after 20 min of ultrasonication in water.

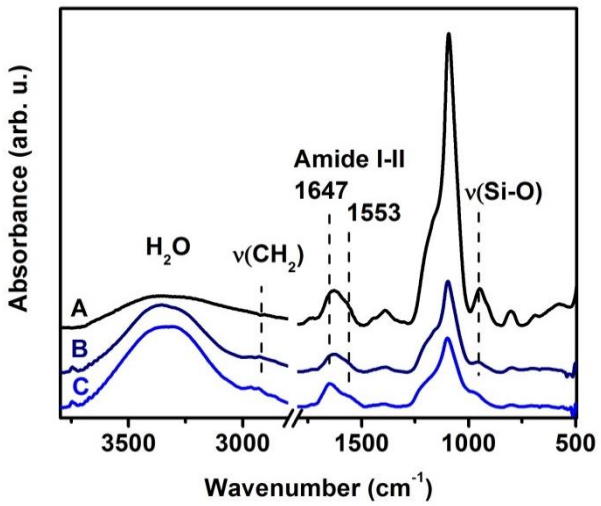

Fig.S-7 FTIR analysis of CN particles (A), after 14-days dissolution test in total cell medium (B), and in saline (C).

***In vitro* labeling and follow-up**

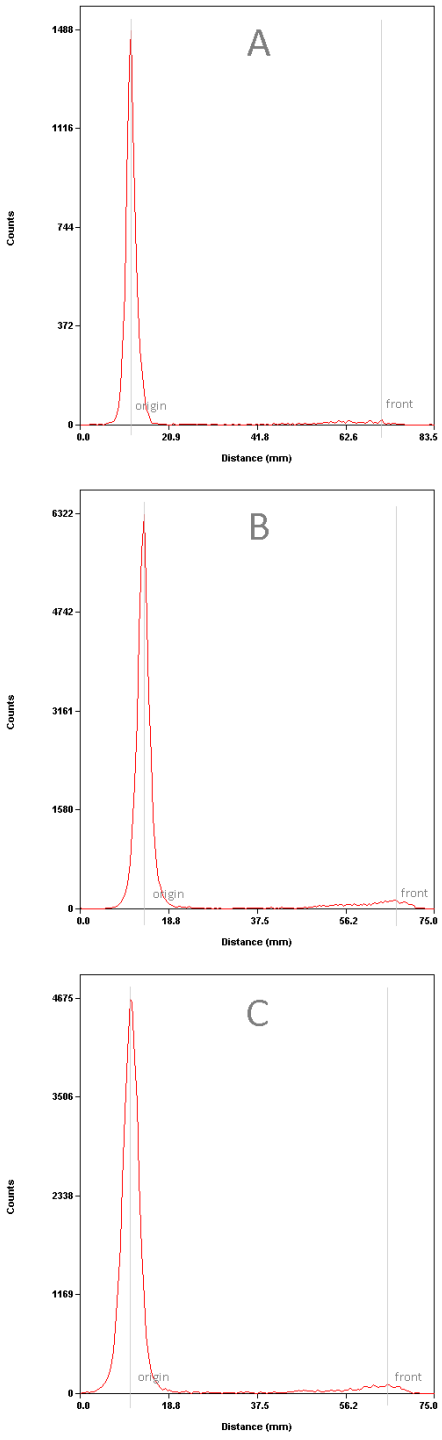

Fig.S-8 TLC chromatograms of ^{99m}Tc-labeled CN nanoparticles. A: 30 min B: 3 hours C: 20 hours in PBS postlabelling. ^{99m}Tc-labeled CN NPs remain at origin while free ^{99m}Tc-pertechnetate stands out with the solvent front.

***In vivo* biodistribution**

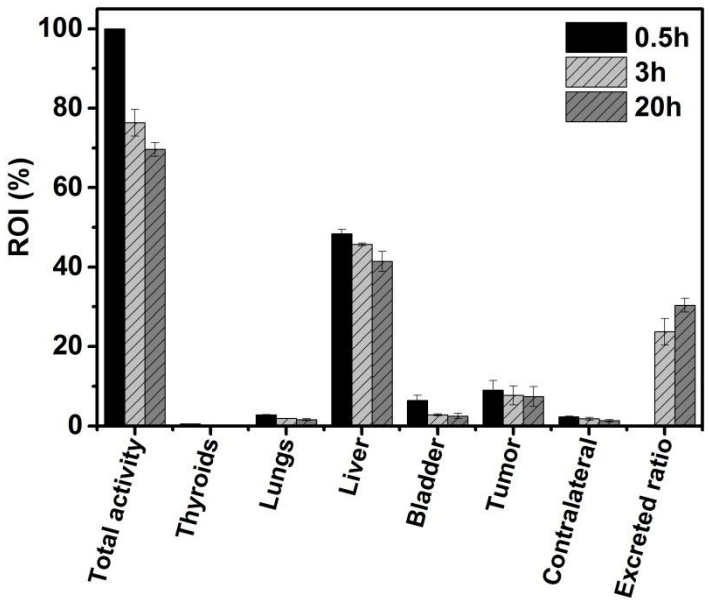

Fig.S-9 Injected dose per whole organ percentages (I.D.%) of a He/De tumour transplanted Fisher rats at different time intervals after ^{99m}Tc-labelled nanocarrier i.v. injections.